# INDOOR AIR POLLUTION ESTIMATES AT A CITY-WIDE SCALE IN BARCELONA

Author: Andreu Julian Izquierdo
Supervisors: Jan Mateu Armengol[1,3] and Cristina Carnerero Quintero[1]
Tutor: Raül Marcos Matamoros[2]
[1] *Barcelona Supercomputing Center (BSC), Barcelona, Spain*
[2] *Facultat de Física, Universitat de Barcelona, Diagonal 645, 08028 Barcelona, Spain. and*
[3] *Department of Fluid Mechanics, Universitat Politècnica de Catalunya, Barcelona, Spain**

**Abstract:** Urban air quality presents a significant global environmental challenge. In this context, understanding indoor and outdoor air quality levels is key to assessing population exposure better. Despite extensive research on modeling and monitoring air quality, studies that simultaneously model both remain limited. This study addresses this gap by combining Nitrogen Dioxide ($NO_2$) outdoor levels from the CALIOPE-Urban air quality model with indoor-outdoor parametric relations. Bias-corrected $NO_2$ concentration levels at the street scale are used. These $NO_2$ levels are based on a kriging data-fusion method, merging monitoring station data and the CALIOPE-Urban dispersion model. Two parametric relations depending on building use are assessed for deriving indoor air quality levels: infiltration rates and indoor-outdoor ratios. Bias-corrected outdoor levels and the parametric relations are combined to obtain unprecedented city-wide maps containing indoor $NO_2$ concentrations accounting for uncertainty quantification. Despite large confidence intervals in our results, the validation against observational data shows satisfactory model performance. Results reveal significant variations in indoor $NO_2$ concentrations across different districts, with the highest levels observed in areas with heavy traffic such as the l'Eixample district. Specifically, in this area, 86.4% of homes have a probability of 50% or higher of exceeding the legal threshold of 40 $\mu g/m^3$, posing considerable health risks for their inhabitants. This comprehensive approach refines the understanding of indoor and outdoor air quality dynamics in Barcelona, revealing $NO_2$ pollution hotspots and enabling reliable and comprehensive air pollution exposure studies.

## I. INTRODUCTION

The impact of air pollution on human health has become a major problem in cities due to high pollution levels and the increasing percentage of people living in urban areas. Currently, more than half of the world's population resides in cities, with even higher percentages in regions such as Europe, where over 70% live in urban areas (European Environment Agency 2024). According to the IPCC, this trend is expected to continue growing in the coming years (IPCC 2021). Focusing on the city of Barcelona, $NO_2$ is one of the main pollutants (Generalitat de Catalunya 2021), as a result of high levels of traffic along the city, being motorized transport one of the main sources of outdoor $NO_2$ in urban conurbations (Mohammadi and Calautit 2022). $NO_2$ is an irritant gas that can cause both acute and chronic respiratory effects, including inflammation of the airways (Valero et al. 2009). In 2021, the European Environment Agency (EEA) estimated 52,000 deaths to nitrogen dioxide due to exceeding the 2021 World Health Organization (WHO) annual limits (Chen et al. 2024), (EEA 2023). Furthermore, early-life exposure to indoor $NO_2$ has been negatively associated with neuropsychological development during the first four years of life (Morales et al. 2009). In this context, understanding and monitoring exposure levels in urban areas is a relevant matter to protect public health.

Traditionally, fixed air quality stations have been employed to monitor outdoor pollution levels. However, analyzing human exposure requires a different approach, as individuals spend a major portion of their time indoors. It is estimated that people now spend about 90% of their lives indoors (Milner et al. 2011). To address indoor exposure, studies have increasingly focused on monitoring indoor air quality, particularly in environments such as schools, due to the high sensitivity of children (Rivas et al. 2014, Salonen et al. 2019). Data on indoor pollutant concentrations remain relatively deficient in other environments. Nonetheless, indoor $NO_2$ concentrations can be related to outdoor $NO_2$ levels due to the exchange of air between the two environments (Mohammadi and Calautit 2022, Morawska et al. 2017). Several studies have reported infiltration rate (IR), which accounts for the amount of pollutants penetrating indoors, and the ratio between indoor and outdoor concentration levels (I/O), which also account for indoor emission sources. For instance, Óscar García-Algar and Pichini (2003) reported I/O ratios by analyzing indoor sources of $NO_2$ in the city of Barcelona with passive dosimeters, considering a cohort of 340 infants. They established I/O rations as a function of various factors of indoor sources, such as gas fire, type of extractor fan used during cooking, and the type of central cooking. Following this line, Esplugues et al. (2010) added not only indoor sources to analyze Indoor/Outdoor (I/O) ratios, but also socioeconomic variables in a cohort in València. These included educational level, social class, or smoking habits.

* Electronic address: ajuliaiz22@alumnes.ub.edu

All these studies are based on experimental data by simultaneously measuring indoor and outdoor concentration levels. However, there are also approaches based on computational fluid dynamics (CFD) models to solve the Navier-Stokes equations. Such approaches provide meaningful simulation results on how pollutants disperse in complex geometries. For example, (Mohammadi and Calautit 2022) simulated an ideal canyon, which is a simplified representation of a street used to study environmental factors. They examined the differences in indoor concentration in terms of ventilation, wind speed, and room orientation in a building of three stages. In the same line, Santiago et al. (2022) studied the indoor-outdoor ratio differences taking into account the height of the building and the stage of each room studied.

In this study we aim to develop and validate a method for estimating indoor nitrogen dioxide levels by using literature parametric relations that connect indoor and outdoor concentrations. As input for our methodology, we use the outdoor $NO_2$ concentrations computed through the urban air quality system CALIOPE-Urban (Benavides et al. 2019) and bias-corrected using observational data (Criado et al. 2023). We analyse infiltrated and indoor $NO_2$ across Barcelona city during 2019. We carefully consider uncertainty sources coming from the outdoor $NO_2$ data and the used parametric relations. Our final goal is to enhance the understanding of $NO_2$ exposure within indoor environments in Barcelona.

## II. DATA AND METHODOLOGY

### A. Domain of study

Barcelona is a city located on the Mediterranean coast, in the northeast of the Iberian Peninsula. It is the capital of Catalonia and the second most populous city in Spain, with a population of 1.6 million inhabitants, a surface area of 101.4 $km^2$ and a population density of 16.3 inhabitants per $km^2$ (IDESCAT. Institut d'Estadística de Catalunya 2024). The administrative area is divided into 10 districts (Figure 1). The city has a Mediterranean climate, with mild winters and hot summers, and it is known for its sunny weather and pleasant temperatures. Barcelona is also known for its environmental initiatives, including efforts to reduce air pollution and promote sustainable transportation (Rodriguez-Rey et al. 2022). Barcelona's port is also one of the busiest in the Mediterranean, with a large number of ships and cargo passing through the city each year, which constitutes a significant source of air pollution (Toscano 2023). It is the city in Europe with the highest density of vehicles, leading to increased pollution levels (Rivas et al. 2014).

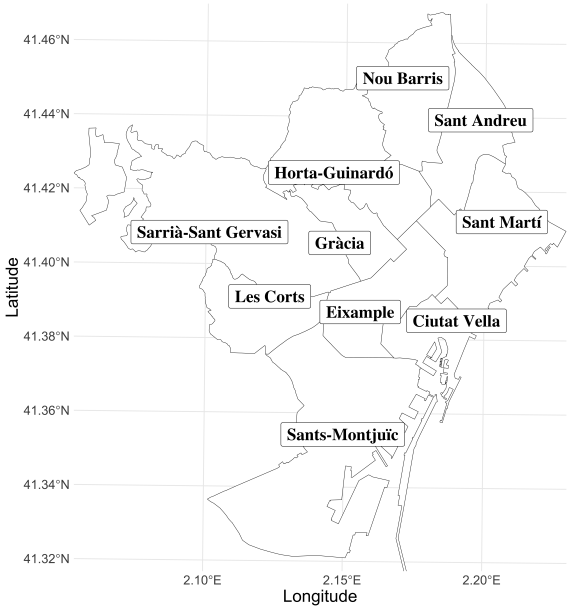


Figure 1: Districts of Barcelona

### B. Data

The data used in this work is divided into two main categories: the outdoor $NO_2$ concentration and the indoor-outdoor ratios.

The outdoor $NO_2$ concentration is obtained from the CALIOPE-Urban model, developed by the Barcelona Supercomputing Center (BSC). This multi-scale air quality system produces hourly estimates of $NO_2$ surface concentrations over Barcelona, coupling the regional air quality system CALIOPE (Baldasano Recio et al. 2011) with the Gaussian dispersion model R-LINE adapted to street canyons. The regional model uses a set of three nested domains for dynamic downscaling: the European region, the Iberian Peninsula, and Catalonia. Furthermore, urban results are bias-corrected using a data-fusion technique that merges model outputs with measurements from the Catalan Air Pollution Monitoring and Forecasting Network (XVPCA) and short experimental campaigns. This provides reliable high-resolution maps of outdoor surface concentration levels of $NO_2$ over Barcelona at a resolution of 20 x 20 meters at 3 meters height (Criado et al. 2023). For the aim of this study, the annual and the seasonal means of 2019 are used. Criado et al. (2023) also made available the $NO_2$ uncertainty, which will allow us to estimate indoor $NO_2$ uncertainties and to evaluate probability of exceeding the legal thresholds.

Apart from the outdoor $NO_2$ concentration, two well-established parameters in the literature are considered. On the one hand, the infiltration rate, which quantifies the fraction of outdoor $NO_2$ that contributes to indoor concentration levels. It typically depends on three parameters: the penetration coefficient, which is defined

as the fraction of $NO_2$ that passes through the building walls, the air change rate, and the deposition rate. In the case of $NO_2$, the penetration coefficient is considered to be 1 (Hu and Zhau 2020), as the entire fraction of $NO_2$ in the outdoor air mass, fully enters indoors. Consequently, the infiltration factor mainly depends on the ventilation patterns (Mohammadi and Calautit 2022, Morawska et al. 2017).

On the other hand, the I/O ratio is defined as the fraction of the indoor and outdoor concentrations of $NO_2$. Its expression is described in Equation 1.

$$I/O = \frac{C_{indoor}}{C_{outdoor}} \tag{1}$$

So, the infiltration rate is equal to the I/O ratio when there are no indoor sources. These values could be obtained from measuring campaigns or from Computational Fluid Dynamics (CFD) models. In this work, the values are obtained from Hu and Zhau (2020), a review of 218 studies reporting measuring campaigns from several countries. The review identified three different indoor environments: homes, schools, and workplaces, and categorized them into three periods in the year. This is because their emission sources and ventilation patterns may differ. The infiltration rates used are shown in Table I and the I/O rates in Table II.

Table I: Seasonal Infiltration rates for three different indoor environments.

| | Homes | Offices | Schools |
|---|---|---|---|
| Summer | $0.87 \pm 0.13$ | $0.81 \pm 0.05$ | $0.89 \pm 0.22$ |
| Winter | $0.63 \pm 0.25$ | $0.72 \pm 0.17$ | $0.75 \pm 0.20$ |
| Spring and Fall | $0.65 \pm 0.24$ | $0.64 \pm 0.12$ | $0.72 \pm 0.22$ |

Moving forward, we use the Copernicus Urban Atlas 2018 (EEA 2021) to distinguish between homes and workplaces. This Atlas provides land use and land cover data from satellite images at high resolution for Europe, including the city of Barcelona. For the schools' locations, we use the information available on the council dataset website (Ajuntament de Barcelona 2019), covering kindergartens, schools, high schools, and universities.

Finally, to validate our results, we use two different measurement campaigns: xAire and Breath. These campaigns provide simultaneous indoor and outdoor $NO_2$ concentration data for schools in the city of Barcelona.

The first one, xAire citizen science campaign (Perelló et al. 2021) in 2017 was composed of 725 passive samplers distributed across 23 schools in the city of Barcelona. A passive sampler is a device that absorbs pollutants directly from the surrounding air without requiring a power supply, allowing for easy and inexpensive monitoring over a wide area. Outdoors samplers were located in the school surroundings or in the playground within the school. The second experimental campaign, Breath (Sunyer et al. 2015), deployed samplers in 39 schools during 2012 and 2013.

### C. Methodology

This section aims to describe the data analysis and processing methods applied to the available $NO_2$ outdoor data. The first step is to establish a coherent value of indoor-outdoor rates with the data we are applying. The indoor-outdoor rates depend on building characteristics, indoor sources (e.g., gas cooking or heating), and people's behavior. Therefore, the ratios vary greatly in different campaigns across different countries, even when measuring in the same environment type. Because of this, we select only European and Mediterranean-basin countries detailed in Annex I.

The final values that we use for the I/O ratio are shown in Table II. The means are calculated using the averages of all I/O values from the mentioned campaigns. The standard deviation shown in the table is calculated as the mean of the standard deviation instead of an error correlation, given that we wanted to account for the dispersion of the mean value. Such dispersion is expected as I/O rates embraces very different indoor air quality contexts.

Table II: Mean Indoor - Outdoor ratios for the Mediterranean basin and their standard deviation.

| | Homes | Work | Schools |
|---|---|---|---|
| I/O ratio | $0.98 \pm 0.77$ | $0.73 \pm 0.24$ | $0.92 \pm 0.51$ |

For the infiltration rate, a different analysis was done. Since this parameter is independent of the indoor sources, all the measurement campaigns were considered for its calculation. Moreover, to have a better representation of this rate, a seasonal distinction was made. We considered three different infiltration factors, one for winter (December to March) and summer (June to September), and a third for spring & fall (April, May, October, and November), each ensuring an equal number of days throughout the different subsets. This will help in the discussion of the results, as the ventilation patterns change during the year.

A land use map of the city of Barcelona is used to distinguish between homes, schools, and workplaces. This specific information is not easily available, nor in the literature or on the council dataset website. To categorize homes and workplaces, the time-microenvironment-activity (TMA) methodology was applied (Ramacher and Karl 2020). This approach involves associating various microenvironments with the Land Use and Land Cover (LULC) of the Copernicus Urban Atlas 2018 product (EEA 2021) based on satellite imagery. LULC distinguishes between roads, industrial areas, port areas, green areas, water bodies, and urban fabric. The TMA allows the identification of workplaces and home microenvironments in any European urban region where Urban Atlas data is accessible.

The procedure is the following: First, the Urban Atlas file is cropped within the limits of Barcelona, as it

contains information about the entire metropolitan area. Next, for each different category described in the Urban Atlas, we applied the proposed building use distribution (Ramacher et al. 2019). For the "continuous urban fabric" category, it is proposed to allocate 70% to residential buildings and 30% to workplaces. This distribution ensures that office buildings and commercial areas in the densely populated city center are represented. The remaining "urban fabric" are designated as homes. Lastly, categories such as "industrial, commercial, public, military, and public units" as well as "construction sites" are classified as workplaces.

Once we have a city-wide map of land use in Barcelona, the output data of the CALIOPE-Urban model is used to assign outdoor NO2 concentrations to each building. This consists of superposing the 20 m × 20 m grid of the annualized CALIOPE-Urban model with the land use map. To do so, the centroid of each block of the land use map is calculated. Then, the $NO_2$ concentration of the CALIOPE-Urban model is interpolated following an Ordinary Kriging to the corresponding block. With this, we obtain the outdoor $NO_2$ concentration for each block of the city with their corresponding variance.

The next step is to apply the parametric relations to obtain indoor $NO_2$ concentration levels. For this, the I/O ratio is applied to the blocks of homes, schools, and workplaces. To quantify the uncertainty of the indoor $NO_2$ concentration, we combine the standard deviation of outdoor $NO_2$ from CALIOPE-Urban with the indoor-outdoor ratios (and infiltration ratios) with Equation 2.

$$\sigma^2_{[NO_2]_I} = \left(\sigma^2_{I/O} + \mu^2_{I/O}\right)\left(\sigma^2_{[NO_2]_O} + \mu^2_{[NO_2]_O}\right) - \mu^2_{I/O}\mu^2_{[NO_2]_O} \quad (2)$$

where $\sigma$ is the standard deviation, $\mu$ is the mean, and $[NO_2]_I$ and $[NO_2]_O$ are the indoor and outdoor concentration, respectively. Finally, the indoor $NO_2$ concentration is obtained by multiplying the outdoor concentration by the I/O ratio.

A validation of the results is performed using the measurement campaigns data, xAire and Breath. First, to compare observational data from different years with the 2019 CALIOPE-Urban output, we normalized the data using a method from Perelló et al. (2021). This method assumes independency regardless of location and can be uniformly applied to all sampling devices. Although this might introduce some variability into the experimental data, it compensates for biases due to metorological factors (such as wind speed, atmospheric stability, precipitation, radiation, and temperature), and enables the integration of data from both campaigns (Criado et al. 2023). The adjusted factor is calculated for each month and year of measurements. It is defined by Equation 3, where $NO_{2,\text{measured, month}}$ is the measurement taken in a particular month, $NO_{2,2019}$ is the annual average of all stations in 2019, and $NO_{2,\text{month}}$ is the monthly average of all stations for the given month.

$$F = NO_{2,measured,month}\frac{NO_{2,2019}}{NO_{2,month}} \quad (3)$$

To analyze if legal $NO_2$ limit values are being exceeded in Barcelona we study two variables: the percentage of blocks that have an associated $NO_2$ indoor levels above the allowed threshold and the likelihood that the $NO_2$ concentration will surpass this limit, calculating the probability of exceedance.

First, we compute the amount of blocks exceeding the limit value of $NO_2$ concentration. Additionally, we estimate the probability of exceeding a given threshold, assuming a normal distribution for the $NO_2$ error. Considering that, $L$ is the established limit, $Z(x)$ is the $NO_2$ concentration, $\sigma(x)$ is the standard deviation, and $F$ is the cumulative distribution function of the normal distribution; then, the probability of exceedance (P(X)) of each block x is shown in Equation 4.

$$P(x) = 1 - F\left(\frac{L - Z(x)}{\sigma(x)}\right) \quad (4)$$

Two different thresholds are considered: $40\mu g/m^3$, which is the annual limit value for $NO_2$ set by the European Air Quality Directive 2008/50/EC (EC 2008); and the limit of 20 $\mu g/m^3$ that is expected to be established soon (Parliament 2024).

All data processing, methodology development, and results are achieved using R coding. Additionally, the maps displayed in the results section are created using the ggplot2 package (Wickham 2016) in R.

## III. RESULTS AND DISCUSSION

### A. Indoor air quality levels in Barcelona

Figure 2 shows the outdoor $NO_2$ concentration assigned to each block of buildings. This is the first step before applying the parametric relationships of indoor-outdoor rates and obtaining an indoor value for each block. As expected, buildings next to the main streets carrying high dense traffic are those with a higher associated outdoor $NO_2$ concentration.

Once we apply the ratios for each environment, we obtain a map for the indoor air quality of $NO_2$ concentration levels. It is shown in Figure 3a along with the associated standard deviation and the normalized standard deviation (Figures 3b and 3c, respectively). The results are similar to the outdoor concentration ones but with some differences to point out. The concentration has generally been reduced by about 10 % for residences and schools, and about 30 % for workplaces, consistent with the rates applied. This is more visible in the work blocks in the city center (l'Eixample district) where the indoor $NO_2$ is higher than in other districts. Moreover,


Figure 2: Outdoor $NO_2$ concentration associated to each block.

the results enable the identification of hot spots. These are located mainly in the city center with high traffic intensity roads and associated with the highest density zones in the city.

Diving into the uncertainties analysis, we have two main components. On the one hand, the one associated with the outdoor concentration. This value is an estimation of the error variance of the universal kriging technique and decreases in places near a monitoring station. On the other hand, the high dispersion of the indoor-outdoor rates, and its consequent high standard deviation (especially for homes), induces a considerable dispersion of the results. The greater the concentration, the greater the associated dispersion. The larger standard deviation in residences is because natural ventilation is predominant in these environments, and therefore, the dispersion is larger. Other reasons include variations in building characteristics that influence airflow and temperature regulation (Morawska et al. 2017). Looking at the Eixample district, building blocks located next to each other have very different standard deviations. This is because, unlike residences, workplaces' I/O ratio have a smaller standard deviation and its dissemination of values is lower. This fact is most clearly shown in the normalized standard deviation. While residences have around 50-60 % of scattering, depending on the neighborhood; the dispersion of work blocks and, to a lesser extent, schools, is around 20-30 %

Another aspect to consider is that we did not take into account additional variables (e.g. gas cook or socioeconomic differences) that could potentially change the I/O ratios, which were studied in some articles (Esplugues et al. 2010), (Óscar García-Algar and Pichini 2003). We made this decision because of the lack of data availability.

### B. Probabilities of exceedance

After obtaining a city-wide map of the indoor air quality, we can assess if the legal limit set by the Directive 2008/50/EC is being exceeded. To do so, firstly, we evaluate how many blocks are actually above the 40 $\mu g/m^3$ of $NO_2$. To have a better knowledge of how pollution is distributed in the city, the blocks are categorized by districts and by type of environment. These results are shown in Table III.

Table III: Number of blocks exceeding and the percentage (in parenthesis) exceeding the annual limit values set by Directive 2008/50/EC by districts and environments.

| | Exceedances of the legal thereshold | | |
|---|---|---|---|
| **District** | **Homes** | **Schools** | **Work** |
| Ciutat Vella | 180 (45.6%) | 19 (46.3%) | 13 (5.2%) |
| Eixample | **317 (86.4%)** | **61 (66.3%)** | 43 (7.2%) |
| Gràcia | 126 (13.1%) | 5 (12.8%) | 11 (7.2%) |
| Horta-Guinardó | 120 (5.7%) | 1 (2.9%) | 11 (0.8%) |
| Les Corts | 133 (18.4%) | 2 (3.8%) | 11 (4.5%) |
| Nou Barris | 99 (7.4%) | 2 (4.9%) | 1 (0.4%) |
| Sant Andreu | 118 (21.4%) | 1 (2.1%) | 11 (3.1%) |
| Sant Martí | 242 (22.6%) | 2 (3.6%) | 19 (3.5%) |
| Sants-Montjuïc | 129 (26.3%) | 6 (18.2%) | 20 (1.7%) |
| Sarrià-Sant Gervasi | 494 (35.5%) | 8 (36.2%) | 28 (17.7%) |
| Barcelona | 1958 (18.2%) | 107 (22.5%) | 160 (4.1%) |

In general, residential buildings have higher percentages, followed by schools and work buildings. As observed in the indoor $NO_2$ maps of Figure 3, the most polluted zones are in the city center, specifically in *Eixample* and *Ciutat Vella* districts. The most affected area is Eixample, where nearly 9 out of 10 residential blocks exceed the legal threshold. Additionally, over 65 % of educational centers in Eixample have indoor $NO_2$ concentrations above the limit. However, looking at the workplaces, these blocks do not exhibit the same behavior. This is because there are no significant $NO_2$ sources in these areas, and mechanical ventilation with filtration systems is predominant. Looking at the results for the entire city, schools overall have a higher percentage than residences, even though residences are more numerous. Like in the district's analysis, workplaces have a lower percentage of blocks exceeding the legal threshold.

To compute the dispersion associated with $NO_2$ concentrations in this analysis, we calculate the probability of exceedance per block, assuming a normal distribution. The city map is represented in Figure 4. Again, the higher exceedances are located in the Eixample, with

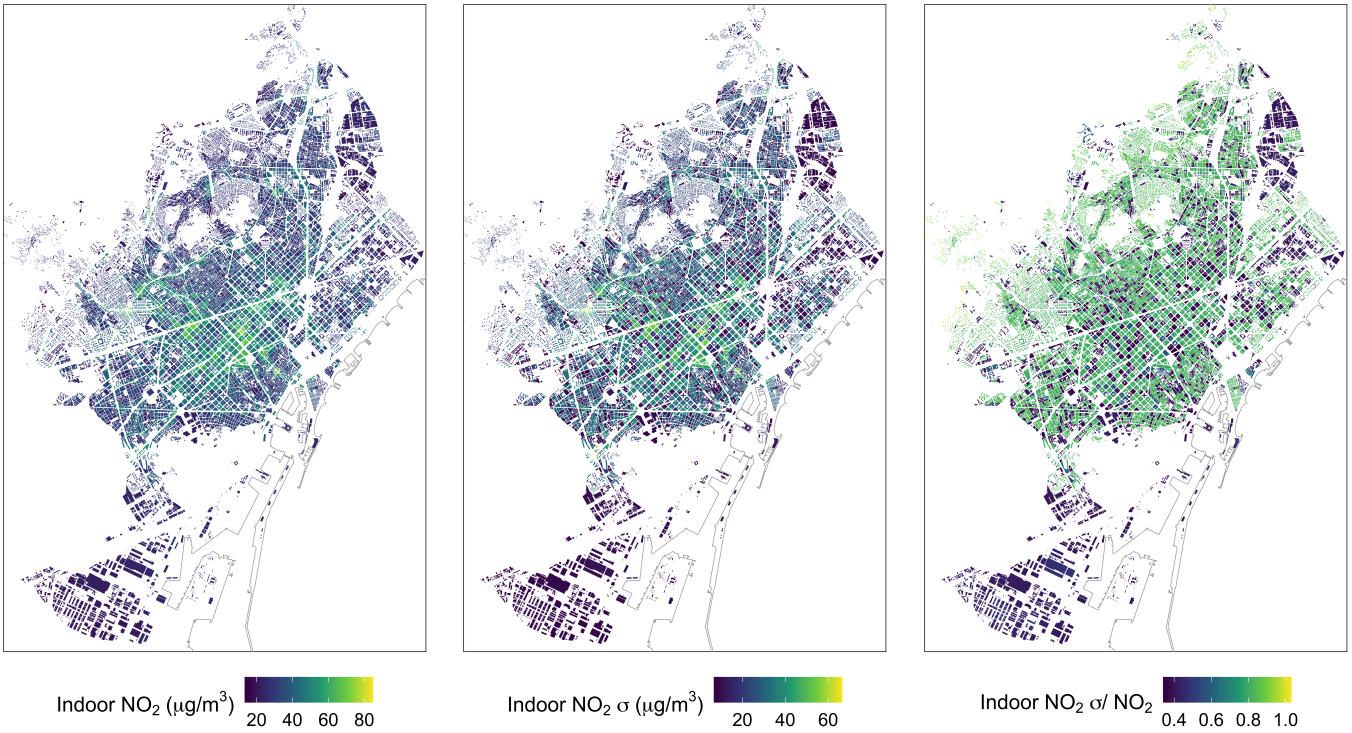


(a) $NO_2$ (b) $\sigma_{NO_2}$ (c) $\sigma_{NO_2}/NO_2$

Figure 3: Indoor $NO_2$ results per building block: in (a) is represented the $NO_2$ concentration, in (b) its standard deviation, and in (c) the normalized standard deviation.

some areas exceeding 70 % of the probability of exceedance of 40 $\mu g/m^3$.

The results show that 15 % of them exceed the 50 % probability of exceedance of the threshold set by Directive 2008/50/EC, mostly in the Eixample district with a 70 % of exceedance. Furthermore, the European Commission is expected to tighten the thresholds to be more similar to those of the World Health Organization. With that horizon in mind, the new directive will come into effect this year or next, but the limit of 20 µg/m³ must be met starting from 2030. For this new threshold, the probability of exceedances rises to 97 % of the blocks in the city exceeding 50 % of probability (37 % for the 75 % probabilities). Given these results, it is clear that this issue constitutes a public health problem. Therefore, it is recommended to implement policies to reduce these figures. Non-compliance with these policies could result in fines for the responsible administrations.

### C. Infiltration rate

Given the high levels of $NO_2$ concentration in the Eixample district, in this section we are studying its origin, whether it is due to the high pollutant situation outdoors or the indoor sources also play a role. To extend this analysis, we consider applying the infiltration rates (see table I) to this district. This way, we are obtaining which fraction of pollutant enters from the outdoors to the indoor environments. Given that this rate strongly depends on the ventilation patterns, and these change during the different seasons of the year, we consider three different maps (summer, winter, and spring & fall). The results (Figure 5) indicate that approximately 70% of the indoor concentration levels originate from outdoor sources. Regarding seasonal differences, the period of the year with the highest infiltration of $NO_2$ into buildings is summer. Contrary to what might be thought, as indoor spaces are less polluted than outdoors, opening more windows allows higher concentrations of NO2 to enter the buildings, despite increased recirculation and air renewal. Taking into account that the input of the outdoor data is lower for spring & fall seasons, the worst season in terms of indoor pollution is summer. The observed difference between winter and spring/fall can be attributed to higher overall outdoor concentration levels in winter, likely due to more stable meteorological conditions.

Regarding the spatial distribution, the highest levels are located in the major city center streets, like Passeig de Gràcia and Aragó streets, where cars and other motor vehicles dominate. In these zones, opening a window significantly increases the concentration of pollutants in the indoor space, especially in residences, where manual

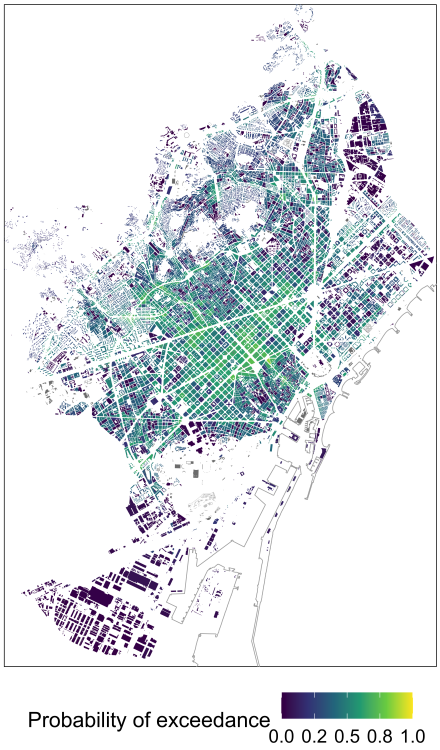


Figure 4: Probability of normal exceedance of 40 $\mu g/m^3$ $NO_2$ limit value per building block.

ventilation dominates in front of mechanical ventilation.

Furthermore, we estimate the mixture distribution of indoor $NO_2$ for each environment in the Eixample district (Figure 6). The mixture distribution quantifies the probability density based on all mean values in the Eixample and their associated variance. To compute it, we follow a Monte Carlo approach: first, a building block is randomly selected; then, an indoor NO2 value is drawn assuming a normal distribution based on the corresponding mean and variance of the specific block. This procedure is repeated $10^6$ times for each environment (work, school, and home). Finally, densities are calculated from this subset only retaining positive values to obtain unique distributions for each environment.

Thus, we are obtaining the indoor concentration distribution by computing in addition the intrinsic variance of each block. Assuming a higher dispersion of I/O ratio for schools and homes, their distributions are flatter in comparison to workplaces. The mean of the distribution indicates that only in work buildings the 40 $\mu g/m^3$ legal threshold is not exceeded. Both schools and homes have their maximum above that threshold.

### D. Validation of results

Finally, using available data from two experimental campaigns, we validate our indoor $NO_2$ results. These campaigns reported data of simultaneous indoor and outdoor $NO_2$ levels for 62 schools in Barcelona. Figure 7 represents the indoor results of our methodology versus measured indoor concentrations. The associated standard deviation of our predicted values is also represented. A dashed line represents the 1:1 ratio. An estimated error of 25 % is considered for the measurements (Hafkenscheid et al. 2009).

Our results slightly overestimated the indoor concentration, as the majority of the schools are a bit above the dashed line. To quantify these biases, the root mean square error (RMSE) is calculated. Distinguishing between campaigns, Breathe has an RMSE of 15.5 $\mu g/m^3$, while xAire is a bit lower with 10.8 $\mu g/m^3$. We also computed the linear regression correlation coefficient for each campaign having the following results: $R^2_{Breath} = 0.27$ and $R^2_{xAire} = 0.55$. The root mean square error results are coherent with this $R^2$ results, as the deviation between the measurements and our predictions for Breath are 5 $\mu g/m^3$ higher than for the xAire campaign. For both campaigns, our methodology overestimates the indoor concentration levels. One reason for this could be the calculating method of the indoor-outdoor rates, as this work includes Mediterranean basin countries that might have different schools' characteristics, impacting the measurement of indoor $NO_2$ concentration. It is also important to note that indoor concentration may not be uniform. The measured indoor concentration depends on the particular point where the sampler is installed.

Likewise, it is important to point out that xAire campaign was conducted over two months while Breathe recorded data throughout a whole year. This is the reason for the dispersion of the measures between campaigns and reflected in the $R^2$ results. As we apply a single value of the I/O ratio for the whole year, we expect seasonal biases to some extent. xAire results follow better our predictions as the measurements were taken in February and March. However, for Breath, our method overestimated some cases, mainly in fall when the outdoor concentration is lower and the ventilation is reduced.

Considering the high dispersion observed in both schools and homes, this deviation is already accounted for in the estimated standard deviation of schools. Thus, we find the method's performance satisfactory.

## IV. CONCLUSIONS

This study offers a groundbreaking analysis of Barcelona's indoor air quality by examining $NO_2$ concentration levels across the city for three different indoor environments: schools, residences, and workplaces. Understanding pollution levels in indoor environments is a step forward for more accurate human exposure assessment to pollution. By integrating outdoor $NO_2$ data from the CALIOPE-Urban model with indoor-outdoor parametric relationships, we have obtained the indoor concentration per building block.

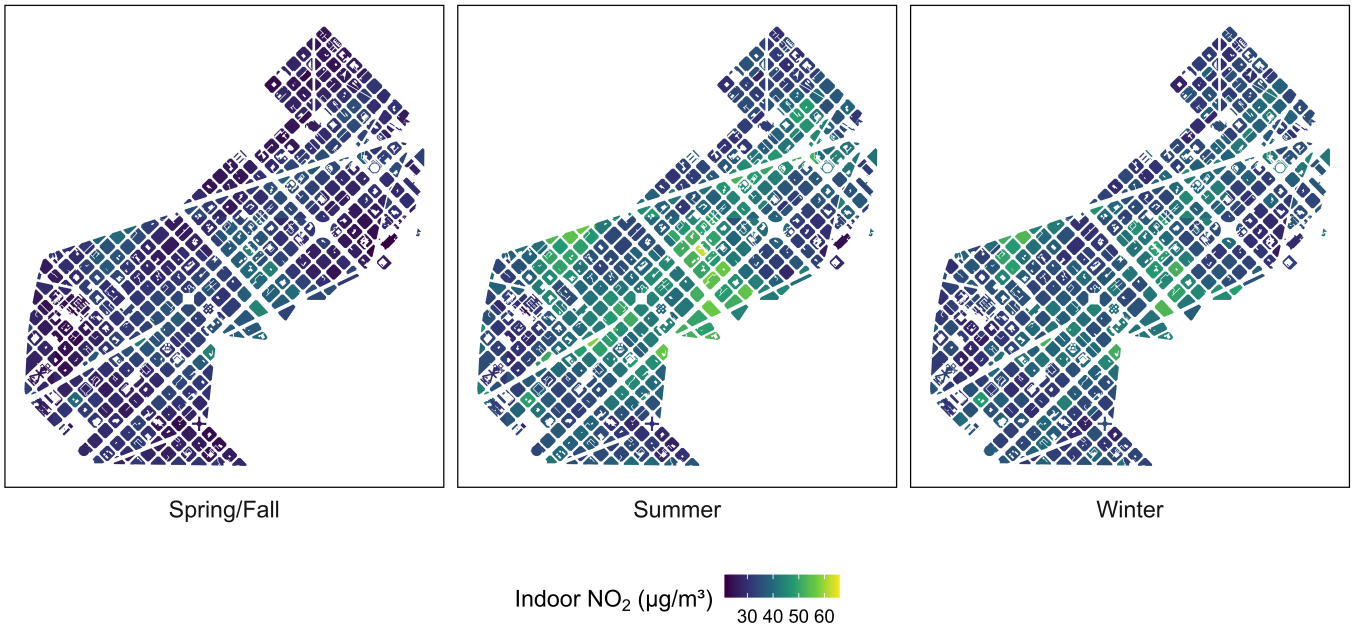


Figure 5: Infiltrated indoor $NO_2$ by seasons.

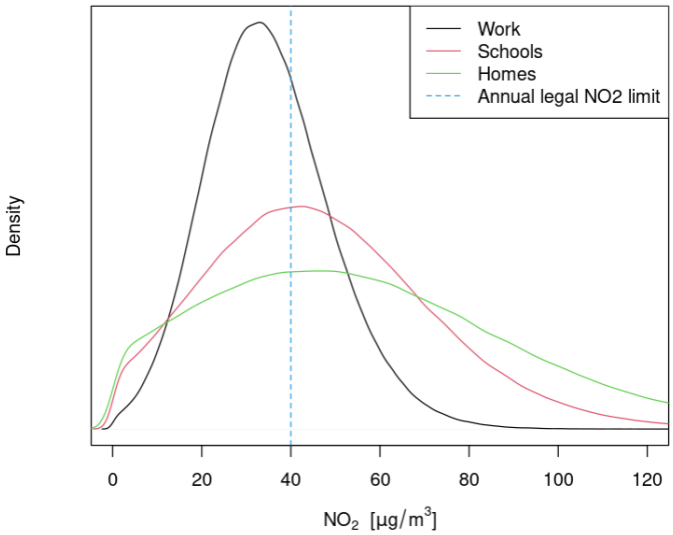


Figure 6: Mixture distribution probability for l'Eixample district.

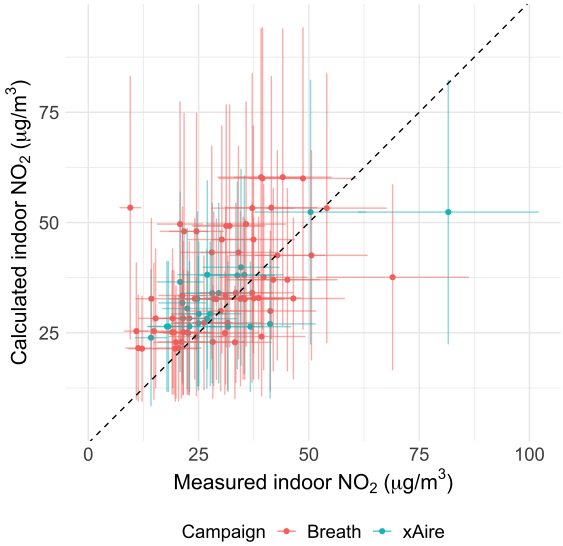


Figure 7: Indoor $NO_2$ schools validation. In red is represented Breath campaign and in blue xAire. Along the concentration values are represented their associated standard deviation. In addition, the dashed line represents the ratio equal to 1.

The findings revealed significant variations in indoor $NO_2$ concentrations across different districts and types of environments. The highest levels were observed in areas with heavy traffic, such as the l'Eixample district, particularly in residences and schools. Seasonal variations also played a critical role, with summer showing the highest infiltration rates due to increased ventilation. This seasonal impact underscores the importance of considering temporal changes in air quality studies and raising awareness among citizens about the ventilation consequences in polluted areas.

Furthermore, the validation of results using data from the xAire and Breath campaigns showed satisfactory performance of the methodology, despite some overestimation in indoor concentrations.

The analysis of the probability of exceedances revealed that a substantial fraction of residential blocks and schools, especially in densely populated districts, have critical $NO_2$ concentration values. Particularly, we

estimate that more than 86% of residences and 66% of schools in Eixample are exposed to $NO_2$ levels above the legal threshold.

These findings stress the importance of implementing specific air quality improvement policies to prevent considerable health risks to citizens. The characterization of indoor air quality in schools and the rest of the environments could be improved with more studies and campaigns of simultaneously indoor and outdoor measures centered in Barcelona to have a bigger acknowledgment of the dispersion in indoor and outdoor rates.

In future research, it is important to focus on improving both indoor and outdoor air quality measurements and to explore how socioeconomic factors impact air quality. It is essential to consider the associated uncertainties in these efforts and the validation of residences and workplaces. Enhancing the precision of exposure assessments will aid in the development of effective strategies to reduce public health risks in urban areas. Additionally, an interesting research direction would involve estimating the population in the analysis. Having knowledge of the number of residents in a residential block, the workforce in a particular workplace, or the number of students in a school would enhance exposure studies and better inform the implementation of air quality policies.

In conclusion, this study advances our understanding of indoor air pollution in Barcelona, providing a framework for assessing population exposure to $NO_2$ and informing public health interventions. Further research and continuous monitoring are essential to address the challenges of urban air quality and protect the health of city inhabitants.

## ACKNOWLEDGMENTS

I want to express my deep appreciation to my supervisors, Jan Mateu and Cristina Carnerero, and my tutor, Raül Marcos, for their invaluable guidance and support throughout this research. I also deeply appreciate the Earth Sciences Department at the Barcelona Supercomputing Center for the opportunity to collaborate with their esteemed team members. Finally, I want to express my appreciation to Sofia and my family for their encouragement and support.

## REFERENCES

Ajuntament de Barcelona. Open Data BCN. `https://opendata-ajuntament.barcelona.cat/data/es/dataset/educacio-ensenyament-reglat`, 2019. Accessed: 2 April 2024, under license Creative Commons by 4.0.

J. M. Baldasano Recio, M. T. Pay Pérez, O. Jorba, S. Gassó, and P. Jiménez-Guerrero. An annual assessment of air quality with the caliope modeling system over spain. *Science of the Total Environment*, 409:2163–2178, 2011. doi: 10.1016/j.scitotenv.2011.01.041.

J. Benavides, M. Snyder, M. Guevara, A. Soret, C. Pérez García-Pando, F. Amato, X. Querol, and O. Jorba. Caliope-urban v1.0: coupling r-line with a mesoscale air quality modelling system for urban air quality forecasts over barcelona city (spain). *Geoscientific Model Development*, 12(7):2811–2835, 2019. doi:10.5194/gmd-12-2811-2019. URL `https://gmd.copernicus.org/articles/12/2811/2019/`.

Z. Y. Chen, H. Petetin, R. F. Méndez Turrubiates, and et al. Population exposure to multiple air pollutants and its compound episodes in europe. *Nature Communications*, 15: 2094, 2024. doi:10.1038/s41467-024-46103-3.

Alvaro Criado, Jan Mateu Armengol, Hervé Petetin, Daniel Rodriguez-Rey, Jaime Benavides, Marc Guevara, Carlos Pérez García-Pando, Albert Soret, and Oriol Jorba. Data fusion uncertainty-enabled methods to map street-scale hourly no2 in barcelona: a case study with caliope-urban v1.0. *Geoscientific Model Development*, 16(8):2193–2213, April 2023. ISSN 1991-959X. doi:10.5194/gmd-16-2193-2023.

EC. *Directive 2008/50/EC of the European Parliament and of the Council of 21 May 2008 on ambient air quality and cleaner air for Europe.* 2008. URL `http://data.europa.eu/eli/dir/2008/50/2015-09-18/eng`. Legislative Body: $OP_DATPRO$.

EEA. Urban atlas land cover/land use 2018 (vector), July 2021. URL `https://doi.org/10.2909/fb4dffa1-6ceb-4cc0-8372-1ed354c285e6`.

EEA. Harm to human health from air pollution in europe: burden of disease 2023. `https://www.eea.europa.eu/publications/harm-to-human-health-from-air-pollution/`, 2023.

Ana Esplugues, Ferran Ballester, M Estarlich, Sabrina Llop, Virginia Fuentes-Leonarte, and E Mantilla. Indoor and outdoor concentrations and determinants of no2 in a cohort of 1-year-old children in valencia, spain. *Indoor air*, 20: 213–23, June 2010. doi:10.1111/j.1600-0668.2010.00646.x.

European Environment Agency. Exceedance of air quality standards. `https://www.eea.europa.eu/en/analysis/indicators/exceedance-of-air-quality-standards`, 2024. Accessed: June 2024.

Generalitat de Catalunya. La qualitat de l'aire a catalunya - anuari 2019, 2021. URL `chrome-extension://efaidnbmnnnibpcajpcglclefindmkaj/https://mediambient.gencat.cat/web/.content/home/ambits_dactuacio/atmosfera/qualitat_de_laire/avaluacio/balancos_i_informes/documentos/La-qualitat-de-laire-a-Catalunya-2019.pdf`. Accessed: June 2024.

T. Hafkenscheid, A. Fromage-Marriette, E. Goelen, M. Hangartner, U. Pfeffer, H. Plaisance, F. De Santis, K. Saunders, W. Swaans, S. Tang, J. Targa, and M. Gerboles. Review of the application of diffusive samplers for the measurement of nitrogen dioxide in ambient air in the european union. EUR 23793 EN JRC51106, OPOCE, Luxembourg (Luxembourg), 2009.

Hu and Zhau. Relationship between indoor and outdoor $NO_2$. *Journal name*, 180:Page numbers, 2020. doi: 10.1016/j.buildenv.2020.106909.

IDESCAT. Institut d'Estadística de Catalunya. Idescat. institut d'estadística de catalunya [internet], 2024. URL `http://www.idescat.cat`. Accessed: 2024.

IPCC. 8 urban systems and other settlements. `https://www.ipcc.ch/report/ar6/wg3/chapter/chapter-8/`, 2021. IPCC AR6 WGIII Chapter08, "Over half of the world's population currently resides in urban areas – a number forecasted to increase to nearly 70% by 2050.".

J. Milner, S. Vardoulakis, Z. Chalabi, and P. Wilkinson. Modelling inhalation exposure to combustion-related air pollutants in residential buildings: Application to health impact assessment. *Environment International*, 37:268–279, 2011. doi:10.1016/j.envint.2010.08.019.

Murtaza Mohammadi and John Calautit. Quantifying the transmission of outdoor pollutants into the indoor environment and vice versa—review of influencing factors, methods, challenges and future direction. *Sustainability*, 14(1717):10880, January 2022. ISSN 2071-1050. doi: 10.3390/su141710880.

E. Morales, J. Julvez, M. Torrent, R. de Cid, M. Guxens, M. Bustamante, and et al. Association of early-life exposure to household gas appliances and indoor nitrogen dioxide with cognition and attention behavior in preschoolers. *American Journal of Epidemiology*, 169:1327–1336, 2009. doi:10.1093/aje/kwp067.

L. Morawska, G. A. Ayoko, G. N. Bae, G. Buonanno, C. Y. H. Chao, S. Clifford, S. C. Fu, O. Hänninen, C. He, C. Isaxon, M. Mazaheri, T. Salthammer, M. S. Waring, and A. Wierzbicka. Airborne particles in indoor environment of homes, schools, offices and aged care facilities: The main routes of exposure. *Environment International*, 108:75–83, November 2017. ISSN 0160-4120. doi: 10.1016/j.envint.2017.07.025.

European Parliament. Air pollution: Deal with council to improve air quality, 2024. URL `chrome-extension://efaidnbmnnnibpcajpcglclefindmkaj/https://www.europarl.europa.eu/pdfs/news/expert/2024/2/press_release/20240219IPR17816/20240219IPR17816_en.pdf`.

J. Perelló, A. Cigarini, J. Vicens, I. Bonhoure, D. Rojas-Rueda, M. J. Nieuwenhuijsen, M. Cirach, C. Daher, J. Targa, and A. Ripoll. Large-scale citizen science provides high-resolution nitrogen dioxide values and health impact while enhancing community knowledge and collective action. *Science of the Total Environment*, 789:147750, 2021. doi:10.1016/j.scitotenv.2021.147750.

M. O. P. Ramacher, M. Karl, J. Bieser, J.-P. Jalkanen, and L. Johansson. Urban population exposure to $NO_x$ emissions from local shipping in three baltic sea harbour cities - a generic approach. *Atmospheric Chemistry and Physics*, 19(14):9153–9179, 2019. doi:10.5194/acp-19-9153-2019. URL `https://acp.copernicus.org/articles/19/9153/2019/`.

Martin Otto Paul Ramacher and Matthias Karl. Integrating modes of transport in a dynamic modelling approach to evaluate population exposure to ambient $NO_2$ and $PM_{2.5}$ pollution in urban areas. *International Journal of Environmental Research and Public Health*, 17(6), 2020. ISSN 1660-4601. doi:10.3390/ijerph17062099. URL `https://www.mdpi.com/1660-4601/17/6/2099`.

I. Rivas, M. Viana, T. Moreno, M. Pandolfi, F. Amato, C. Reche, L. Bouso, M. Àlvarez Pedrerol, A. Alastuey, J. Sunyer, and X. Querol. Child exposure to indoor and outdoor air pollutants in schools in barcelona, spain. *Environment International*, 69:200–212, August 2014. ISSN 0160-4120. doi:10.1016/j.envint.2014.04.009.

Daniel Rodriguez-Rey, Marc Guevara, Mª. Paz Linares, Josep Casanovas, Jan M. Armengol, Jaime Benavides, Albert Soret, Oriol Jorba, Carles Tena, and Carlos Pérez García-Pando. To what extent the traffic restriction policies applied in barcelona city can improve its air quality? *Science of The Total Environment*, 807:150743, 2022. ISSN 0048-9697. doi: https://doi.org/10.1016/j.scitotenv.2021.150743. URL `https://www.sciencedirect.com/science/article/pii/S0048969721058216`.

Heidi Salonen, Tunga Salthammer, and Lidia Morawska. Human exposure to no2 in school and office indoor environments. *Environment International*, 130:104887, September 2019. ISSN 0160-4120. doi:10.1016/j.envint.2019.05.081.

Jose Santiago, Esther Rivas, Riccardo Buccolieri, Alberto Martilli, Marta García Vivanco, Rafael Borge, Oliver Carlo, and Fernando Martin. Indoor-outdoor pollutant concentration modelling: a comprehensive urban air quality and exposure assessment. *Air Quality, Atmosphere Health*, 15, 05 2022. doi:10.1007/s11869-022-01204-0.

J. Sunyer, M. Esnaola, M. Alvarez-Pedrerol, and et al. Association between traffic-related air pollution in schools and cognitive development in primary school children: a prospective cohort study. *PLoS Medicine*, 12(3):e1001792, 2015. doi:10.1371/journal.pmed.1001792. PMC - PubMed.

Domenico Toscano. The impact of shipping on air quality in the port cities of the mediterranean area: A review. *Atmosphere*, 14(7), 2023. ISSN 2073-4433. doi: 10.3390/atmos14071180. URL `https://www.mdpi.com/2073-4433/14/7/1180`.

Natalia Valero, Inmaculada Aguilera, Sabrina Llop, Ana Esplugues, Audrey de Nazelle, Ferran Ballester, and Jordi Sunyer. Concentrations and determinants of outdoor, indoor and personal nitrogen dioxide in pregnant women from two spanish birth cohorts. *Environment International*, 35(8):1196–1201, November 2009. ISSN 0160-4120. doi: 10.1016/j.envint.2009.08.002.

Hadley Wickham. *ggplot2: Elegant Graphics for Data Analysis*. Springer-Verlag New York, 2016. ISBN 978-3-319-24277-4. URL `https://ggplot2.tidyverse.org`.

Cecilia Figueroa Oriol Vall Xavier Basagaña Jordi Sunyer Assumpcio Freixa Xavier Guardino Óscar García-Algar, Meritxell Zapater and Simona Pichini. Sources and concentrations of indoor nitrogen dioxide in barcelona, spain. *Journal of the Air & Waste Management Association*, 53(11):1312–1317, 2003. doi:10.1080/10473289.2003.10466297. URL `https://doi.org/10.1080/10473289.2003.10466297`.

## V. ANNEX I

Residences

| Nationality | N | n | Mean | SD |
|---|---|---|---|---|
| Belgium | 1 | 19 | 0.85 | 0.25 |
| Bulgaria | 1 | 20 | 2.42 | 5.04 |
| Croatia | 1 | 15 | 0.60 | 0.00 |
| Czech Rep. | 1 | 50 | 0.97 | 0.00 |
| Denmark | 1 | 38 | 0.73 | 0.12 |
| Finland | 4 | 414 | 0.67 | 0.15 |
| France | 3 | 178 | 0.49 | 0.24 |
| Germany | 3 | 1954 | 0.56 | 0.16 |
| Greece | 1 | 3 | 0.79 | 0.34 |
| Italy | 6 | 800 | 1.22 | 1.51 |
| Netherlands | 4 | 1607 | 1.36 | 0.93 |
| Norway | 1 | 30 | 0.70 | 0.00 |
| Poland | 1 | 14 | 0.80 | 0.00 |
| Portugal | 1 | 4 | 0.38 | 0.25 |
| Slovakia | 1 | 20 | 1.31 | 0.00 |
| Spain | 4 | 1621 | 1.34 | 0.49 |
| Sweden | 5 | 466 | 0.77 | 0.30 |
| Switzerland | 9 | 1832 | 0.74 | 0.21 |
| Turkey | 2 | 73 | 1.45 | 0.70 |
| UK | 9 | 1422 | 1.00 | 0.82 |

Table IV: I/O ratios per country for residences. N is the number of campaigns carried, n is the number of sampling sites and SD is the standard deviation.

Workplaces

| Nationality | N | n | Mean | SD |
|---|---|---|---|---|
| Czech Rep. | 1 | 50 | 0.73 | 0.00 |
| Finland | 1 | 176 | 0.89 | 0.00 |
| France | 2 | 93 | 0.85 | 0.33 |
| Greece | 1 | 4 | 0.66 | 0.00 |
| Ireland | 1 | 3 | 0.14 | 0.08 |
| Italy | 1 | 9 | 0.87 | 0.00 |
| Switzerland | 4 | 240 | 0.79 | 0.22 |
| Turkey | 4 | 21 | 0.90 | 0.35 |
| UK | 4 | 150 | 0.96 | 0.23 |

Table V: I/O ratios per country for workplaces. N is the number of campaigns carried, n is the number of sampling sites and SD is the standard deviation.

Schools

| Nationality | N | n | Mean | SD |
|---|---|---|---|---|
| Belgium | 1 | 54 | 0.83 | 0.29 |
| Croatia | 1 | 6 | 0.77 | 0.21 |
| France | 4 | 154 | 1.38 | 1.78 |
| Greece | 1 | 3 | 0.70 | 0.33 |
| Italy | 1 | 3 | 0.74 | 0.00 |
| Malta | 1 | 15 | 0.62 | 0.00 |
| Netherlands | 5 | 120 | 0.51 | 0.16 |
| Poland | 1 | 2 | 0.54 | 0.26 |
| Portugal | 4 | 98 | 0.85 | 0.67 |
| Serbia | 2 | 40 | 1.45 | 0.71 |
| Spain | 7 | 529 | 1.29 | 0.97 |
| Sweden | 2 | 22 | 1.10 | 0.00 |
| Switzerland | 1 | 2 | 1.06 | 0.03 |
| Turkey | 3 | 14 | 0.96 | 0.24 |
| UK | 4 | 62 | 0.70 | 0.51 |

Table VI: I/O ratios per country for schools. N is the number of campaigns carried, n is the number of sampling sites and SD is the standard deviation.